MEDICAL SENSORS

PROJECT REPORT

PET/CT Image Denoising and Segmentation based on a Multi Observation and Multi Scale Markov Tree Model

November 23, 2016

Yeman Hagos
Vu Hoang Minh

Contents

Chapter 1

Introduction

Image denoising and segmentation are essential step in many advanced techniques of image processing.

Image noise is a random variation of brightness and visible as grains. It may arise by the sensor and circuity of a digital camera during the time of capturing or image transmission that adds spurious and extraneous information [23]. Noise in image is defined as pixels showing false or different intensity values instead of true or expected values. Natural image denoising is a process of reducing or removing noise from an image. In other words, it is defined as a process of estimating an original clean version of noise corrupted image [14].

According to actual image characteristic, noise statistical property and frequency spectrum distribution rule, people have developed many methods of eliminating noises, which approximately are divided into space and transformation fields. the transformations generate some coefficients and then processed. Then the aim of eliminating noise is achieved by inverse transformation, like wavelet transform and contourlet transforms [21][18].Wavelet denoising attempts to remove the noise present in the signal while preserving the signal characteristics, regardless of its frequency content [20].

Image segmentation is an important early vision task where pixels with similar features are grouped into homogeneous regions in which class labels are assigned to each pixels in the image according to the properties of a pixel and neighborhood pixels. It is a joint process of detection and estimation of class labels to each pixels and shapes of homogeneous regions.

These days, Bayesian estimation has become popular method to study the statistical properties of regions of an image to determine the possible number of class labels and to assign pixels to the corresponding label. Most of Bayesian techniques use region models to describe statistics of homogeneous regions of an image. The Markov Random Fields (MRF) has been extensively in use to model the class labels of the pixels in the image. The image is segmented by estimating theMaximum a Posteriori (MAP) orMaximum Likelihood (ML) estimate of the pixels[4] [24].

In this paper, we implemented multi-observation and multi resolution denoising (contourlet and wavelet) and segmentation tumor in Computed Temography (CT) and Positron Emission Tomography

(PET) images.

The paper is organized as follows. In Chapter 2, we introduced about Wavelet Transform (WT), Contourlet Transform (CT), Wavelet Denoising (WD), Contourlet Denoising (CD), Wavelet-Contourlet Denoising (WCD), and Hidden Markov Tree (HMT). Chapter 3 gives the implementation and algorithm of our decisioning and segmentation. Section IV gives the developed method overview. In Chapter 4, we present the denoising and segmentation of CT and PET images, and discussion. Finally, Chapter 5 presents conclusions our implementation.

Chapter 2

Literature Review

2.1 HIDDEN MARKOV TREE

2.1.1 General Introduction

Segmentation of an image into unknown number of distinct and in some way homogeneous regions has been a fundamental issue in low level image analysis. There are many direct application of the algorithm, for example, segmentation of CT, PET, segmentation of Nuclear Magnetic Resonance (NMR) images, and other applications in radar, satellite and agriculture. Many types of approaches has been in practice and in this paper a probabilistic method of segmentation is employed, Hidden Markov Model (HMM) based.

2.1.2 Overview of Hidden Markov Model

The HMT was introduced by Crouse, Nowak and Baraniuk (1998). The context of their work was the modeling of statistical dependencies between wavelet coefficients in signal processing, for which variables are organized in a natural tree structure. Applications of such a model are: image segmentation, signal class cation, denoising and image document categorization [10].

A HMM is a statistical Markov model in which the system being modeled is assumed to be a Markov process with unobserved (hidden) states. In a hidden Markov model, the state is not directly visible, but the output, dependent on the state, is visible. Each state has a probability distribution over the possible output tokens. Therefore, the sequence of tokens generated by an HMM gives some information about the sequence of states. The adjective 'hidden' refers to the state sequence through which the model passes, not to the parameters of the model; the model is still referred to as a 'hidden' Markov model even if these parameters are known exactly [12].

The unifying ideas in using Markov Random Fields for vision are the following:

- Images are dissected into an assembly of nodes that may correspond to pixels.

- Hidden variables associated with the nodes are introduced into a model designed to “explain” the values (colors) of all the pixels.
- A joint probabilistic model is built over the pixel values and the hidden variables
- The direct statistical dependencies between hidden variables are expressed by explicitly grouping hidden variables; these groups are often pairs depicted as edges in a graph.

These properties are illustrated in Figure 2.1 below:

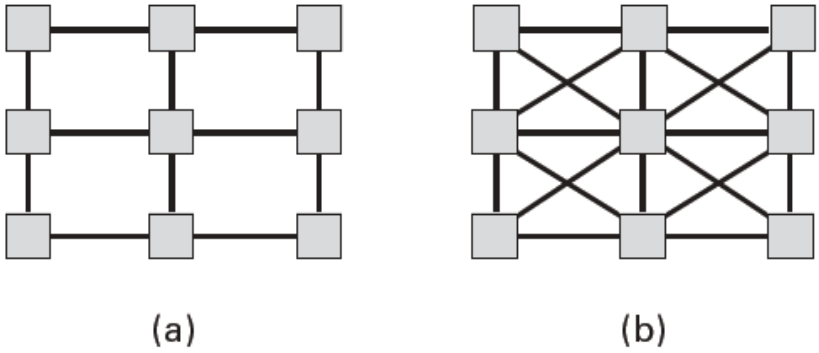

Figure 2.1: Graphs for Markov models in vision. (a) Simple 4-connected grid of image pixels. (b) Grids with greater connectivity here with the 8-connected pixel grid.

The motivation for constructing such a graph is to connect the hidden variables associated with the nodes. For example, for the task of segmenting an image into foreground and background, each node i (pixel) has an associated random variable X_i that may take the value 0 or 1, corresponding to foreground or background, respectively may take the value 0 or 1, corresponding to foreground or background, respectively. In order to represent the tendency of matter to be coherent, neighboring sites are likely to have the same label. So where $(i, j) \in E$, some kind of probabilistic bias needs to be associated with the edge (i, j) such that X_i and X_J tend to have the same label—both 0 or both 1. In fact, any pixels that are nearby, not merely adjacent, are likely to have the same label[12].

123

2.2 DISCRETE WAVELET TRANSFORM

2.2.1 Background

A wavelet is a wave-like oscillation with an amplitude that begins at zero, increases, and then decreases back to zero. It can typically be visualized as a "brief oscillation" like one recorded by a seismograph

or heart monitor [15]. As a mathematical tool, wavelets can be used to extract information from many different kinds of data, including – but certainly not limited to – audio signals and images [16].

In numerical analysis and functional analysis, a Discrete Wavelet Transform (DWT) is any wavelet transform for which the wavelets are discretely sampled. As with other wavelet transforms, a key advantage it has over Fourier Transform (FT) is temporal resolution: it captures both frequency and location information (location in time) [25].

In signal processing, wavelets make it possible to recover weak signals from noise . This has proven useful especially in the processing of X-ray and magnetic-resonance images in medical applications. Images processed in this way can be "cleaned up" without blurring or muddling the details [13].

2.2.2 Discrete Wavelet Transform

In 2-Dimensional dyadic multiresolution, a wavelet orthonormal basis in $L^2(\mathbb{R}^2)$ is built up from (tensor) products involving:

- A scale function φ associated to a multiresolution $\{V_j\}_j \in Z$ of $L^2(\mathbb{R})$
- An orthonormal wavelet $\psi \in L^2(\mathbb{R})$ to define a complete orthonormal system, for the Hilbert space $L^2(\mathbb{R})$ of square integrable functions.

The orthonormal wavelet ψ is constructed as the family of functions:

$$\psi^k_{jn}(x) = 2^{\frac{j}{2}}\psi^k\left(2^j x_1 - n_1, 2^j x_2 - n_2\right) \tag{2.1}$$

for integers $j,k \in \mathbb{Z}$.

For this purpose, one defines three wavelets:

$$\psi^1(x_1,x_2) = \varphi(x_1)\psi(x_2) \tag{2.2a}$$
$$\psi^2(x_1,x_2) = \psi(x_1)\varphi(x_2) \tag{2.2b}$$
$$\psi^3(x_1,x_2) = \varphi(x_1)\varphi(x_2) \tag{2.2c}$$

In the case of the discrete wavelet transform, the mother wavelet is shifted and scaled by powers of two:

$$\psi_{j,k}(t) = \frac{1}{\sqrt{2^j}}\psi\left(\frac{t-k2^j}{2^j}\right) \tag{2.3}$$

where j is the scale parameter and k is the shift parameter, both which are integers.

Recall that the wavelet coefficient γ of a signal $x(t)$ is the projection of $x(t)$ onto a wavelet, and let $x(t)$ be a signal of length 2^N. In the case of a child wavelet in the discrete family above:

$$\gamma_{jk} = \int_{-\infty}^{\infty} x(t)\frac{1}{\sqrt{2^j}}\psi\left(\frac{t-k2^j}{2^j}\right)dt \tag{2.4}$$

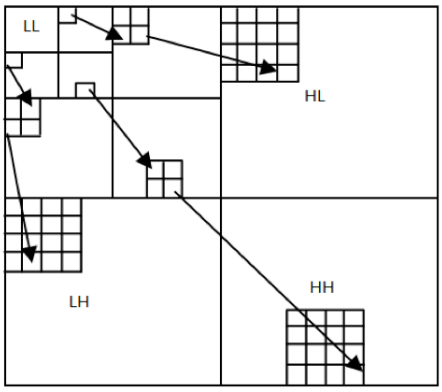

Figure 2.2: Wavelet coefficients arrangement

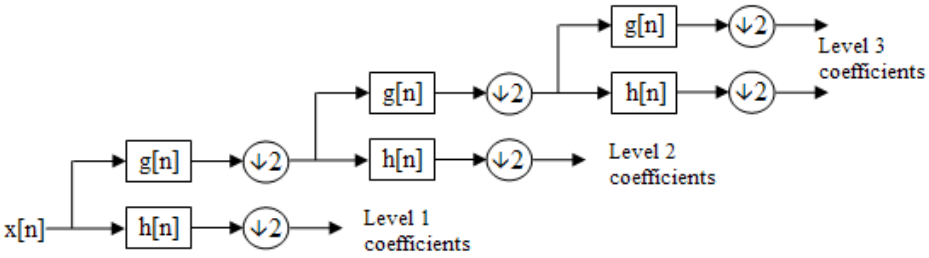

Figure 2.3: A 3 level filter bank

This decomposition, which can be seen in Figure 2.2 [7], is repeated to further increase the frequency resolution and the approximation coefficients decomposed with high and low pass filters and then down-sampled. This is represented as a binary tree with nodes representing a sub-space with a different time-frequency localisation. The tree is known as a filter bank, see Figure 2.3.

2.3 CONTOURLET TRANSFORM

2.3.1 Background

In the field of Geometrical Image Transforms, there are many 1-D transforms designed for detecting or capturing the geometry of image information, such as the FT and WT. However, the ability of 1-D transform processing of the intrinsic geometrical structures, such as smoothness of curves, is limited in one direction, then more powerful representations are required in higher dimensions. The CT, which was proposed in [9], is a new two-dimensional transform method for image representations.

Contourlets form a multiresolution directional tight frame designed to efficiently approximate images made of smooth regions separated by smooth boundaries. The CT has a fast implementation based

on a Laplacian Pyramid (LP) decomposition followed by Directional Filter Banks (DFBs) or Pyramid Directional Filter Banks (PDFBs) applied on each bandpass subband [22]. The new method as proposed in [17] uses a multiscale pyramid that can be adjusted by applying low pass or high pass filters for the different levels.

The LP decomposition only produce one bandpass image in a multidimensional signal processing, that can avoid frequency scrambling. And DFB is only fit for high frequency since it will leak the low frequency of signals in its directional subbands. This is the reason to combine DFB with LP, which is multiscale decomposition and remove the low frequency.

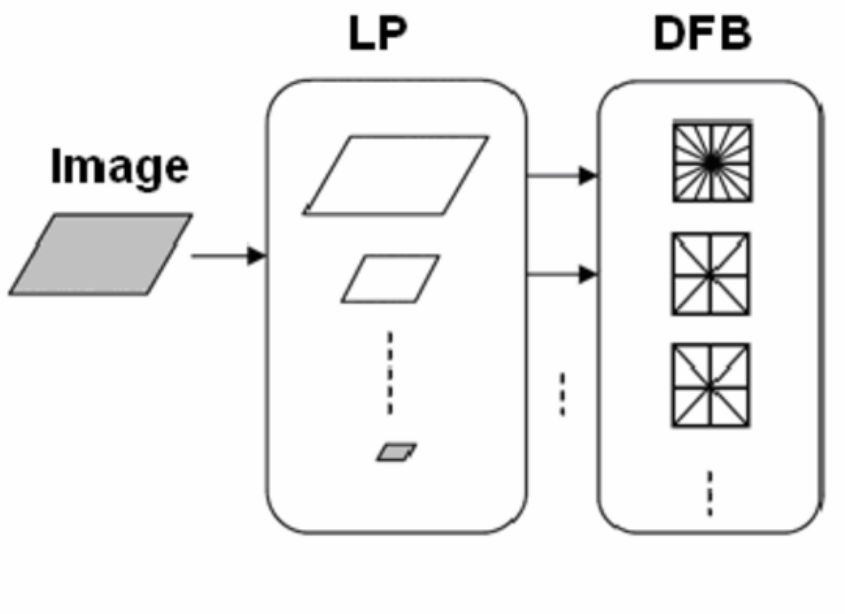

Figure 2.4: Contourlet Transform

2.3.2 Contourlet Transform

The CT is a directional transform, capable of capturing contours and fine details in images. The Figure 2.5 illustrates the CT, in which the input image consists of frequency components like Low Low (LL), Low High (LH), High Low (HL) and High High (HH).

The LP at each level generates a Low pass output (LL) and a Band pass output (LH, HL, and HH). The Band pass output is then passed into DFB, which results in contourlet coefficients. The Low pass output is again passed through the LP to obtain more coefficients and this is done till the fine details of the image are obtained. Figure 2.6 shows the decomposition of brain MR Image.

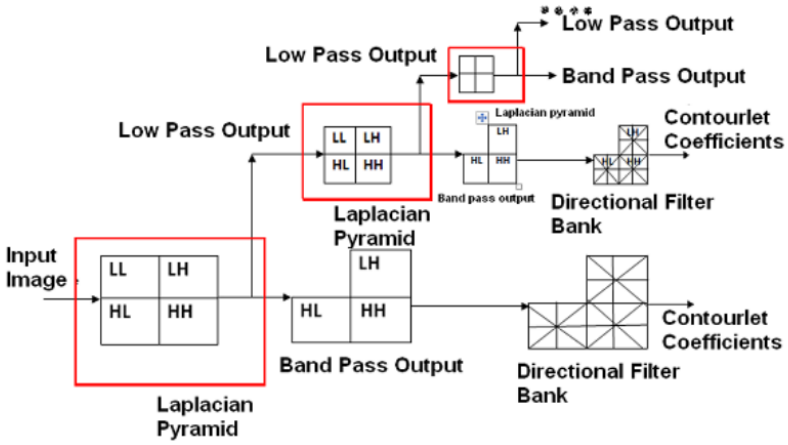

Figure 2.5: Flowchart of Contourlet Transform

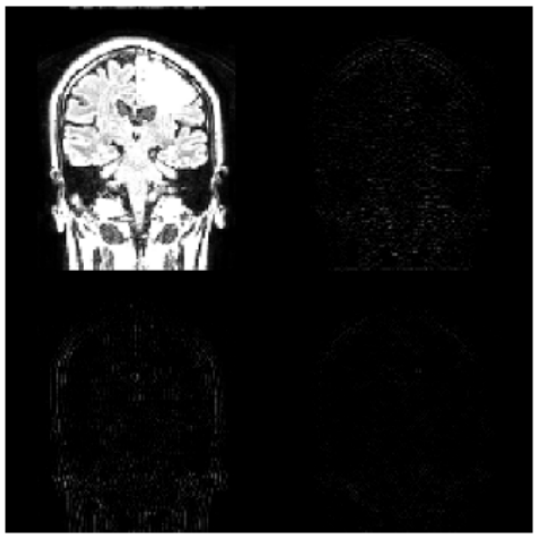

Figure 2.6: Contourlet decomposition of brain MR Image

2.4 PET IMAGE DENOISING

2.4.1 Image Denoising

Image noise is a random variation of brightness and visible as grains. It may arise by the sensor and circuity of a digital camera during the time of capturing or image transmission that adds spurious and extraneous information [23]. Noise in image is defined as pixels showing false or different intensity values instead of true or expected values. Natural image denoising is a process of reducing or removing noise from an image. In other words, it is defined as a process of guesstimating an original clean version of noise corrupted image [14].

The common types of noise that arises in a image are impulse noise (salt-and-pepper noise), amplifier

noise (Gaussian noise), shot noise, quantization noise (uniform noise), film grain, on-isotropic noise, multiplicative noise (speckle noise) and periodic noise. Depending on owning different characteristics, which makes them distinguishable, each type of noise is able to afflict image in different context. As a result, noise reduction filters are developed to minimize the effects of noise in order to ameliorate image processing.

In paper [11], the developed framework was firstly evaluated for PET denoising. In this work the multiobservation aspect of the proposed HMT was exploited in order to associate both Wavelets and Contourlets coefficients to each voxel. An approach combining both CD and WD, namely WCD, was proposed in order to obtain the optimal performance.

2.4.2 PET Image

PET is a nuclear medicine, functional imaging technique that is used to observe metabolic processes in the body. The system detects pairs of gamma rays emitted indirectly by a positron-emitting radionuclide (tracer), which is introduced into the body on a biologically active molecule.

Three-dimensional images of tracer concentration within the body are then constructed by computer analysis. In modern PET-CT scanners, three dimensional imaging is often accomplished with the aid of a CT X-ray scan performed on the patient during the same session, in the same machine.

The examples of PET system and PET brain image can be seen in Figure 2.7.

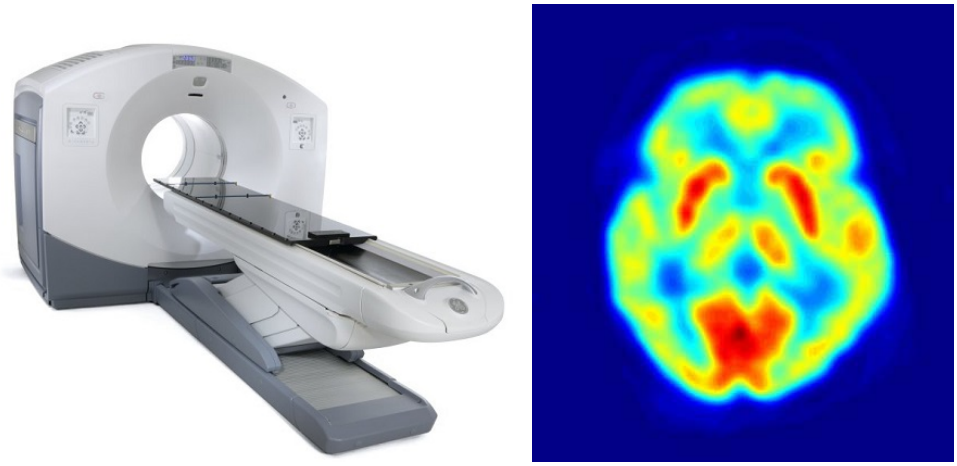

Figure 2.7: PET system and PET brain image

2.4.3 Wavelet and Contourlet Denoising

Wavelet denoising

Wavelet thresholding methods for noise removal, in which the wavelet coefficients are thresholded in order to remove their noisy part, were first introduced by Donoho in 1993 [6]. The theoretical

justifications and arguments in their favour are highly compelling. These methods do not require any particular assumptions about the nature of the signal, permits discontinuities and spatial variation in the signal, and exploits the spatially adaptive multiresolution of the wavelet transform [5].

Contourlet Denoising

The major drawback for wavelets in two-dimensions is their limited ability in capturing directional information. To overcome this deficiency, researchers have recently considered multiscale and directional representations that can capture the intrinsic geometrical structures such as smooth contours in natural images [19].

The primary goal of the contourlet construction is to obtain a sparse expansion for typical images that are piecewise smooth away from smooth contours [9].

Concept of denoising

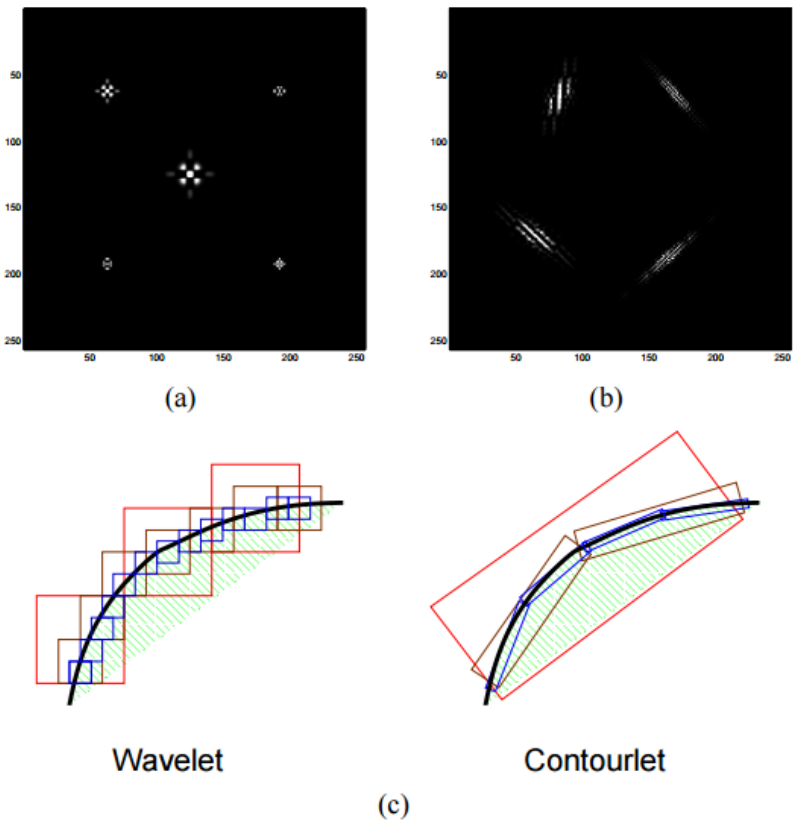

Figure 2.8: Contourlet and wavelet representations for images. (a) Examples of five 2-D wavelet basis images. (b) Examples of four contourlet basis images. (c) Illustration showing how wavelets having square supports that can only capture point discontinuities, whereas contourlets having elongated supports that can capture linear segments of contours, and thus can effectively represent a smooth contour with fewer coefficients.

A more precise explanation of the wavelet denoising procedure can be given as follows. Assume that the observed data is [20]:

$$X(t) = S(t) + N(t) \tag{2.5}$$

where $S(t)$ is the uncorrupted signal with additive noise $N(t)$.

Let $W(\cdot)$ and $W^{-1}(\cdot)$ denote the forward and inverse wavelet transform operators. Let $D(\cdot,\lambda)$ denote the denoising operator with threshold λ.

We intend to denoise $X(t)$ to recover $\hat{S}(t)$ as an estimate of $S(t)$. The procedure can be summarized in three steps:

$$Y = W(X) \tag{2.6a}$$
$$Z = D(Y,\lambda) \tag{2.6b}$$
$$\hat{S} = W^{-1}(Z) \tag{2.6c}$$

while $D(\cdot,\lambda)$ being the thresholding operator and λ being the threshold.

Thresholding

In fact, small coefficients are dominated by noise, while coefficients with a large absolute value carry more signal information than noise. Replacing noisy coefficients (small coefficients below a certain threshold value) by zero and an inverse wavelet transform may lead to a reconstruction that has lesser noise [20].

There are three kinds of thresholding for denoising:

- Hard thresholding
- Soft thresholding
- Universal thresholding

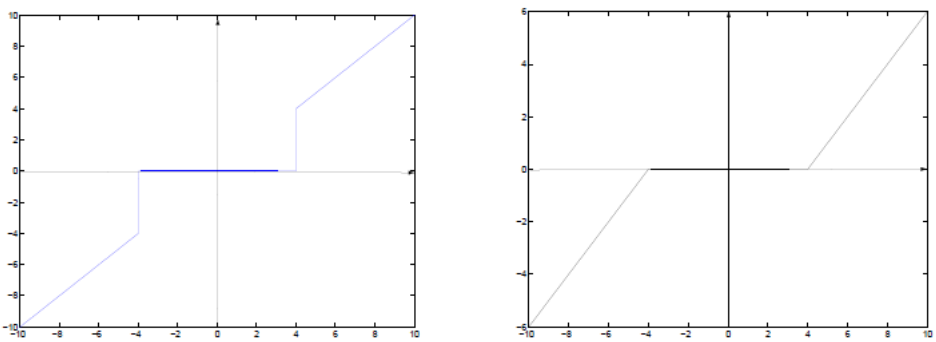

Figure 2.9: Hard and Soft Thresholding

Hard threshold is a "keep or kill" procedure and is more intuitively appealing. The alternative, soft thresholding shrinks coefficients above the threshold in absolute value. See Figure 2.9 for the transfer

functions of hard and soft thresholding, respectively.

The hard thresholding operator is defined as:

$$D(U,\lambda) = \begin{cases} U & \text{for all } |U| > \lambda \\ 0 & \text{otherwise} \end{cases} \tag{2.7}$$

Otherwise, the soft thresholding operator is defined as:

$$D(U,\lambda) = sgn(U)max(0,|U| - \lambda) \tag{2.8}$$

Threshold determination is an important question when denoising. A small threshold may yield a result close to the input, but the result may still be noisy. A large threshold on the other hand, produces a signal with a large number of zero coefficients. This leads to a smooth signal. Paying too much attention to smoothness, however, destroys details and in image processing may cause blur and artifacts [20].

In addition to hard and soft thresholding, a thresholding approach, namely universal thresholding, is introduced:

$$\lambda_{UNIV} = \sqrt{2lnN\sigma} \tag{2.9}$$

where N being the signal length, and σ^2 being the noise variance.

2.4.4 Wavelet-Contourlet Denoising

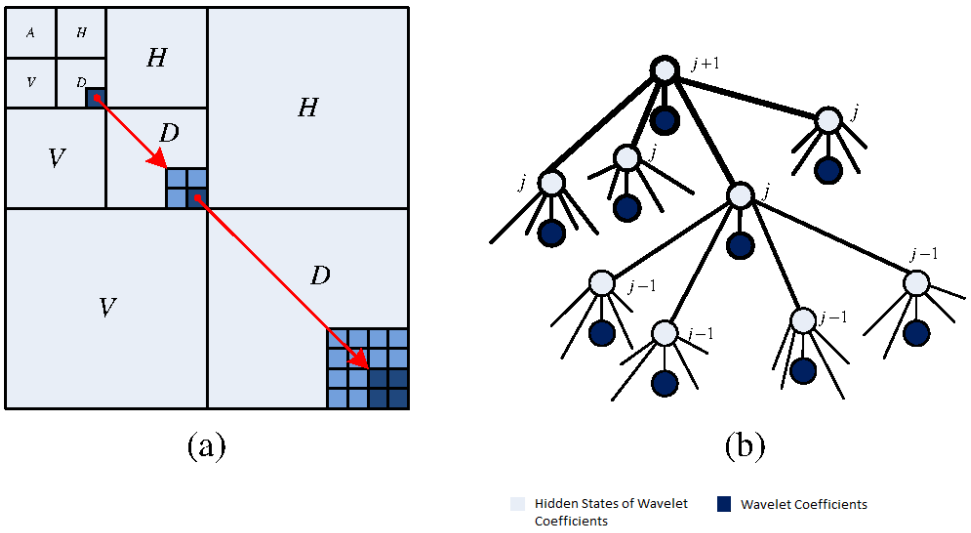

Figure 2.10: Discrete Wavelet Transform and Hidden Markov Tree models

2.4.5 Proposed denoising method: Non-local Means

Non-local means (NL-means) is a linear smoothing technique introduced by Buades et al.. NL-means filtering is an algorithm computing average values of all pixels in the image, which are analyzed how similar they are to the objective pixel. The main difference between NL-means and other filters is the meticulous employment of all possible self-predictions an image is able to provide.

Compared to local filters, which process pixels within a local square window to aim for a reconstruction of the main geometrical configurations, NL-means is more effective in post-filtering intelligibility and preserving details of image and fine structure [3].

2.4.6 Proposed denoising method: Sparse 3D Transform-domain Collaborative Filter

Currently, Sparse 3D Transform-domain Collaborative Filter (BM3D) is a well-known image denoising algorithm introduced by Dabov et al. in 2007 [8]. The basic principles of this algorithm is grouping and collaborative Wiener filtering in two-stage estimations. There is a number of developed algorithms based on the concepts of BM3D; however, BM3D is still the most successful approach, especially for low-SNR PET image.

2.5 PET/CT IMAGE SEGMENTATION

2.5.1 Introduction

Segmentation is the process of splitting an observed image into its homogeneous or constituent regions . Segmentation may also be thought of as labeling process, where each pixel in a given image is assigned a designating the region or class to which it belongs. If the observed image y is defined on a rectangular $M \times N$ lattice Ω, indexed by a pair (i, j) so that $\Omega = (i, j); 1 \leq i \leq Mand 1 \leq j \leq N$ and the label x will be defined on the same label. Thus for each pixel site $s = (s_i, s_j)$ there is a label x_s which specifies to which region the pixel y_s belongs. The relationship between gray scale values and levels is represented by Bayesian Likelihood function. It is modeled by probability distribution of the pixel values, model parameter and the prior distribution of models. Then segmentation is an optimization problem of the labels on entire image[1].

Graph partitioning methods are an effective tools for image segmentation since they model the impact of pixel neighborhoods on a given cluster of pixels or pixel, under the assumption of homogeneity in images. In these methods, the image is modeled as a weighted, undirected graph. Usually a pixel or a group of pixels are associated with nodes and edge weights define the (dis)similarity between the neighborhood pixels. The graph (image) is then partitioned according to a criterion designed to model "good" clusters. Each partition of the nodes (pixels) output from these algorithms are considered an object segment in the image.

MRFs are completely characterized by their prior probability distributions, marginal probability distributions, cliques, smoothing constraint as well as criterion for updating values. The criterion for image segmentation using MRFs is restated as finding the labeling scheme which has maximum probability for a given set of features.

In terms of image segmentation, the function that MRFs seek to maximize is the probability of identifying a labeling scheme given a particular set of features are detected in the image

where Vc(x) is the clique potential and C is the set of all possible cliques. In the image domain, we assume that one pixel has at most 4 neighbors: the pixels in its 4-neighborhood. Then the clique potential is defined on pairs of neighboring pixels

The HMRF-EM framework was first proposed for segmentation of brain MR images [9]. Given an image $Y = (y_1, y_2, ..., y_N)$ where each y_i is the intensity of a pixel, we want to infer a configuration of labels$X = (x_1, x_2, ..., x_N)$ where$x_i \in L$ and L is the set of all possible labels which means the hidden process is a finite valued one(REFERENCE:IMAGE AND SIGNAL RESTORATION USING PAIRWISE MARKOV TREES) In a binary segmentation problem, L = {0,1} . According to the MAP criterion, we seek the labeling x^* which satisfies:

$$X^* = \underset{x}{\operatorname{argmax}}\{\Pr(Y \mid X, \Theta) P(X)\} \tag{2.10}$$

The prior probability $P(X)$ is a Gibbs distribution, and the joint likelihood probability is given by:

$$\begin{aligned} \Pr(Y \mid X, \Theta) &= \prod_i \Pr(y_i \mid X, \Theta) \\ &= \prod_i \Pr(y_i \mid X_i, \theta_{x_i}) \end{aligned} \tag{2.11}$$

where

$$Pr(y_i \mid X_i, \theta_{x_i})$$

is a Gaussian distribution with parameters $\theta_{x_i} = (\mu_{x_i}, \sigma_{x_i})$ and $\Theta = \{\theta_l | l \in L\}$ is the parameter set,which is obtained by the EM algorithm.

2.5.2 EM Algorithm

We use the EM algorithm to estimate the parameter set $\Theta = \{\theta_l | l \in L\}$. We describe the EM algorithm by the following [2]:

1. Start: Assume we have an initial parameter set$\Theta^{(0)}$
2. E-step: At the $t^t h$ iteration, we have $|\Theta^{(t)}$ and we calculate the conditional expectation:

$$Q(\Theta \mid \Theta^{(t)}) = \sum_x \Pr(x \mid Y, \Theta^{(t)}) \ln(\Pr(x, Y \mid \Theta)) \tag{2.12}$$

where $x \in X$, set of all possible configurations of labels.

3. M-step: Now maximize $\Pr(\Theta \mid \Theta^{(t)})$ to obtain the next estimate:

$$\Theta^{(t+1)} == \underset{x}{\operatorname{argmax}}\{\Pr(\Theta \mid \Theta^{(t)})\} \tag{2.13}$$

Then let $\Theta^{(t+1)}$ to $\Theta^{(t)}$ and repeat from the E-step.

The above equations are in general are computationally difficult and here we have assumed the parameters are random processes to simplify our implementation[**?**]. Let $G(z;\theta_l)$ denote a Gaussian distribution function with parameters $\theta_l = (\mu_l, \sigma_l)$:

$$G(z;\theta_l) = \frac{1}{\sqrt{2\pi\sigma^2}} \exp(-\frac{(z-\mu_l)^2}{2\sigma^2}) \tag{2.14}$$

We assume that the prior probability can be written as:

$$P(X) = \frac{1}{Z} \exp(-U(X)) \tag{2.15}$$

where U(X) is the prior energy function. We also assume that

$$\begin{aligned} \Pr(Y \mid X, \Theta) &= \prod_{i=1} \Pr(y_i \mid x_i, \Theta_{x_i}) \\ &= \prod_i G(y_i;\theta_{x_i}) \\ &= \frac{1}{Z'} \exp(-U(Y \mid X) \end{aligned} \tag{2.16}$$

With these assumptions, the HMRF-EM algorithm is given below:

1. Start with initial parameter set $\Theta^{(0)}$.
2. Calculate the likelihood distribution $P^{(t)}(y_i \mid x_i, \theta_{x_i})$.
3. Using current parameter set $\Theta^{(t)}$ to estimate the labels by MAP estimation:

$$\begin{aligned} X^{(t)} &= \underset{x \in X}{\operatorname{argmax}}\{\Pr(Y \mid X, \Theta^{(t)}) P(X)\} \\ &= \underset{x \in X}{\operatorname{argmin}}\{U(Y \mid X, \Theta^{(t)}) + U(X)\} \end{aligned} \tag{2.17}$$

The algorithm for the MAP estimation is discussed below.

4. Calculate the posterior distribution for all $l \in L$ and all pixels y_i:

$$\overset{(t)}{\Pr}(l \mid y_i) = \frac{G(y_i;\theta_i) Pr(l \mid x_{N_i}^{(t)})}{P^{(t)(y_i)}} \tag{2.18}$$

where $x_{N_i}^{(t)}$ is the neighborhood configuration of $x_i^{(t)}$ and

$$P^{(t)}(y_i) = \sum_{l \epsilon L} G(y_i; \theta_i) Pr(l \mid x_{N_i}^{(t)}) \tag{2.19}$$

Note here we have

$$Pr(l \mid x_{N_i}^{(t)}) = \frac{1}{Z} \exp(-\sum_{j \epsilon N_i} V_c(l, x_j^t)) \tag{2.20}$$

5. Use $P^{(t)}(l \mid y_i)$ to update the parameters:

$$\begin{aligned} \mu_l^{(t+1)} &= \frac{\sum_i P^{(t)}(l \mid y_i) y_i}{\sum_i P^{(t)}(l \mid y_i)} \\ (\sigma_l^{(t+1)})^2 &= \frac{\sum_i P^{(t)}(l \mid y_i)(y_i - \mu_l^{t+1})^2}{\sum_i P^{(t)}(l \mid y_i)} \end{aligned} \tag{2.21}$$

2.5.3 MAP Estimation

In the EM algorithm, we need to solve for x? that minimizes the total posterior energy

$$X^* = \underset{x \in X}{\operatorname{argmin}} \{U(Y \mid X, \Theta) + U(X)\} \tag{2.22}$$

with given Y and Θ, where the likelihood energy is

$$\begin{aligned} U(Y \mid X, \Theta) &= \sum_i U(Y_i \mid X_i, \Theta) \\ &= \sum_i (\frac{(y_i - \mu_{x_i})^2}{2\sigma_{x_i}^2} + \ln(\sigma_{x_i})) \end{aligned} \tag{2.23}$$

The prior energy function U(x) has the form

$$U(X) = \sum_{c \epsilon C} V_c(X) \tag{2.24}$$

where $V_c(X)$ is the clique potential and C is the set of all possible cliques.

In the image domain, we assume that one pixel has at most 4 neighbors: the pixels in its 4-neighborhood. Then the clique potential is defined on pairs of neighboring pixels:

$$V_c(x_i, x_j) = \frac{1}{2}(1 - I_{x_i,x_i}) \tag{2.25}$$

Where

$$I_{x_i,x_i} = \begin{cases} 0 & \text{if } x_i \neq x_j \\ 1 & \text{if } x_i = x_j \end{cases} \tag{2.26}$$

We have developed an iterative algorithm to solve (2.22):

1. To start with, we have an initial estimate $X^(0)$, which is from the previous loop of the EM algorithm.
2. Provided $X^{(k)}$, for all $1 \leq i \leq N$, we find

$$X_i^{(k+1)} = \underset{l \in L}{\operatorname{argmin}} \{U(y_i \mid l) + \sum_{j \epsilon N_i} V_c(l, x_j^k))\} \tag{2.27}$$

1. Repeat step 2 until $U(Y \mid X, \Theta) + U(X)$ converges or a maximum k is achieved.

Chapter 3

Implementation

3.1 Coding Standard

3.2 PET Image Denoising

3.2.1 Wavelet Denoising

The procedure of CD is shown in Algorithm 1.

Algorithm 1 Wavelet Denoising

Input: $input\_image$
Output: $denoised\_image$

1: **procedure** waveletdenoising($input\_image$)
2: initialize parameters
3: define vector of numbers of PDFB decomposition levels ▷ $nlevs = [0,0,0,0,0]$
4: decompose PDFB ▷ $y = pdfbdec(input\_image, paras)$
5: convert the output of the PDFB into a vector form ▷ $[c,s] = pdfb2vec(y)$
6: compute threshold ▷ wth
7: compute vector PDFB coefficients ▷ c
8: convert vector form to output structure ▷ $y = vec2pdfb(c,s)$
9: reconstruct $denoised\_image$ ▷ $denoised\_image = pdfbrec(y, paras)$

3.2.2 Contourlet Denoising

The procedure of CD is shown in Algorithm 2.

3.2.3 Wavelet-Contourlet Denoising

The pseudo-code of Non-local means is illustrated in Algorithm 3.

Algorithm 2 Contourlet Denoising

Input: $input\_image$
Output: $denoised\_image$
procedure contourletdenoising($input\_image$)
    initialize parameters
    define vector of numbers of PDFB decomposition levels ▷ $nlevs = [0,0,4,4,5]$
    decompose PDFB ▷ $y = pdfbdec(input\_image, paras)$
    convert the output of the PDFB into a vector form ▷ $[c,s] = pdfb2vec(y)$
    estimate noise standard ▷ $nvar$
    compute threshold ▷ cth
    compute vector PDFB coefficients ▷ c
    convert vector form to output structure ▷ $y = vec2pdfb(c,s)$
    reconstruct $denoised\_image$ ▷ $denoised\_image = pdfbrec(y, paras)$

Algorithm 3 Wavelet-Contourlet Denoising

Input: $input\_image$
Output: $denoised\_image$
procedure waveletcontourletdenoising($input\_image$)
    initialize parameters
    compute waveletdenoising($input\_image$) ▷ w_image
    compute contourletdenoising($input\_image$) ▷ c_image
    for each pixel in $denoised\_image$ **do**
        $denoised\_image(i,j) = mean(w\_image(i,j) + c\_image(i,j))$

3.2.4 Non-local Means Filter

The pseudo-code of Non-local means is illustrated in Algorithm 4.

Algorithm 4 Non-local Means Filter

Input: $input\_image$
Output: $denoised\_image$

```
1:  procedure nlmeans(input_image)
2:      for every pixel in the image do
3:          take a window centered in x with size (2m+1 × 2m+1)
4:          take a window centered in x with size (2n+1 × 2n+1)
5:          for each pixel y in A(x,m) and yx do
6:              compute the difference between W(x,n) and W(y,n)
7:              if w(x,y) > wmax then
8:                  w_max = w(x,y)
9:              compute the average of w(x, y)
10:             compute the sum of weights
11:         give to x the maximum of the other weights
12:         compute total weights
13:         compute the restored value
14:         compute distance
```

3.2.5 Sparse 3D Transform-domain Collaborative Filter

The pseudo-code of Non-local means is illustrated in Algorithm 5.

3.3 PET/CT Image Segmentation

3.4 Graphical User Interface

Algorithm 5 Sparse 3D Transform-domain Collaborative Filter

Input: $input\_image$
Output: $denoised\_image$

procedure bm3dfiltering($input\_image$)
    form blocks
    for each block in the noisy image **do**
        group matched blocks in 3D array group
        keep N^{hard} blocks closest to processed one
    apply 3D isometric linear transform
    apply shrinkage of the transform spectrum
    apply inverse linear transform
    for each block in the noisy image **do**
        basic estimate
        save in buffer
    for each block in basic estimate **do**
        group matched blocks in 3D array group
        keep N^{wien} blocks closest to processed one
    compute Wiener coefficients
    for each block in basic estimate **do**
        final estimate

Chapter 4

Result and Discussion

4.1 Challenges

In unsupervised image segmentation is the process of identifying and detecting the constituent regions of an image, while having no prior knowledge of the number of regions in the image. This problem can be formulated in Bayesian framework, but it needs a lot of optimization.

Chapter 5

Conclusion

Bibliography

[1] Simon A Barker. *Image segmentation using Markov random field models*. PhD thesis, University of Cambridge, 1998.

[2] Laurent Bordes, Didier Chauveau, and Pierre Vandekerkhove. A stochastic em algorithm for a semiparametric mixture model. *Computational Statistics & Data Analysis*, 51(11):5429–5443, 2007.

[3] Antoni Buades, Bartomeu Coll, and J-M Morel. A non-local algorithm for image denoising. In *2005 IEEE Computer Society Conference on Computer Vision and Pattern Recognition (CVPR'05)*, volume 2, pages 60–65. IEEE, 2005.

[4] Hyeokho Choi and Richard G Baraniuk. Image segmentation using wavelet-domain classification. In *SPIE's International Symposium on Optical Science, Engineering, and Instrumentation*, pages 306–320. International Society for Optics and Photonics, 1999.

[5] Rami Cohen. Signal denoising using wavelets. *Project Report, Department of Electrical Engineering Technion, Israel Institute of Technology, Haifa*, 2012.

[6] Ronald R Coifman and David L Donoho. *Translation-invariant de-noising*. Springer, 1995.

[7] Dong Cui, Minmin Liu, Lei Hu, Keju Liu, Yongxin Guo, and Qing Jiao. The application of wavelet-domain hidden markov tree model in diabetic retinal image denoising. *The open biomedical engineering journal*, 9:194, 2015.

[8] Kostadin Dabov, Alessandro Foi, Vladimir Katkovnik, and Karen Egiazarian. Image denoising by sparse 3-d transform-domain collaborative filtering. *IEEE Transactions on image processing*, 16 (8):2080–2095, 2007.

[9] Minh N Do and Martin Vetterli. The contourlet transform: an efficient directional multiresolution image representation. *IEEE Transactions on image processing*, 14(12):2091–2106, 2005.

[10] Jean-Baptiste Durand and Paulo Gonçalves. *Statistical inference for hidden Markov tree models and application to wavelet trees*. PhD thesis, INRIA, 2001.

[11] Houda Hanzouli, Jérôme Lapuyade-Lahorgue, Emmanuel Monfrini, Gaspar Delso, Wojciech Pieczynski, Dimitris Visvikis, and Mathieu Hatt. Pet/ct image denoising and segmentation based on a multi observation and a multi scale markov tree model. In *2013 IEEE Nuclear Science Symposium and Medical Imaging Conference (2013 NSS/MIC)*, pages 1–4. IEEE, 2013.

[12] Gordan Jezic, Yun-Heh Jessica Chen-Burger, Robert J Howlett, and Lakhmi C Jain. Agent and multi-agent systems: Technology and applications.

[13] Tzu-Heng Henry Lee. Wavelet analysis for image processing. 2012.

[14] Anat Levin and Boaz Nadler. Natural image denoising: Optimality and inherent bounds. In *Computer Vision and Pattern Recognition (CVPR), 2011 IEEE Conference on*, pages 2833–2840. IEEE, 2011.

[15] Ariel Lipson, Stephen G Lipson, and Henry Lipson. *Optical physics*. Cambridge University Press, 2010.

[16] Christian Lovis, Brigitte Séroussi, and Arie Hasman. *EHealth-For Continuity of Care: Proceedings of MIE2014*, volume 205. IOS Press, 2014.

[17] Yue Lu and Minh N Do. A new contourlet transform with sharp frequency localization. In *2006 International Conference on Image Processing*, pages 1629–1632. IEEE, 2006.

[18] Boaz Matalon, Michael Elad, and Michael Zibulevsky. Image denoising with the contourlet transform. *Proceedings of SPARSE'05*, 2005.

[19] DD-Y Po and Minh N Do. Directional multiscale modeling of images using the contourlet transform. In *Statistical Signal Processing, 2003 IEEE Workshop on*, pages 262–265. IEEE, 2003.

[20] Raghuram Rangarajan, Ramji Venkataramanan, and Siddharth Shah. Image denoising using wavelets. *Wavelet and Time Frequencies*, 2002.

[21] Sachin D Ruikar and Dharmpal D Doye. Wavelet based image denoising technique. *International Journal of Advanced Computer Science and Applications*, 2(3), 2011.

[22] L Padma Suresh, Subhransu Sekhar Dash, and Bijaya Ketan Panigrahi. Artificial intelligence and evolutionary algorithms in engineering systems. *Proceedings of ICAEES*, 1, 2014.

[23] Rohit Verma and Dr Jahid Ali. A comparative study of various types of image noise and efficient noise removal techniques. *International journal of advanced research in computer science and software engineering*, 3(10):617–622, 2013.

[24] Aurélie Voisin, Vladimir A Krylov, Gabriele Moser, Sebastiano B Serpico, and Josiane Zerubia. Supervised classification of multisensor and multiresolution remote sensing images with a hierarchical copula-based approach. *IEEE Transactions on Geoscience and remote sensing*, 52(6): 3346–3358, 2014.

[25] Jihong Yan. *Machinery Prognostics and Prognosis Oriented Maintenance Management*. John Wiley & Sons, 2014.